Efficiency of ^{123}I-ioflupane SPECT as a marker of basal ganglia damage in acute methanol poisoning: a six-year prospective study

Katerina Kotikova (✉ katerina.kotikova@vfn.cz)

 Toxicological Information Centre, General University Hospital, Prague and Department of Occupational Medicine, First Faculty of Medicine, Charles University Prague

David Zogala

 Institute of Nuclear Medicine, First Faculty of Medicine, Charles University, General University Hospital, Prague

Vaclav Ptacnik

 Institute o Nuclear Medicine, First Faculty o Medicine, Charles University and General University Hospital, Prague

Jiri Trnka

 Institute of Nuclear Medicine, First Faculty of Medicine, Charles University and General University Hospital, Prague

Karel Kupka

 Institute of Nuclear Medicine, First Faculty of Medicine, Charles University and General University Hospital, Prague

Manuela Vaneckova

 Department of Radiology, First Faculty of Medicine, Charles University and General University Hospital, Prague

Zdenek Seidl

 Department of Radiology, First Faculty of Medicine, Charles Universty and General University Hospital, Prague

Pavel Diblik

 Department of Ophtalmology, First Faculty of Medicine, Charles University and General University Hospital, Prague

Jarmila Heissigerova

 Department of Ophtalmology, First Faculty of Medicine, Charles University, and General University Hospital, Prague

Ivan Zak

 Department o Occupational Medicine, First Faculty od Medicine, Charles University and General University Hospital, Prague

Tomas Navratil

Deparment of Occupational Medicine, First Faculty o Medicine, Charles University and General University Hospital, Prague

Martin Komarc

Department of Methodology, Faculty of Physical Education and Sport, Charles University, Prague

Sergey Zakharov

Department of Occupational Medicine, First Faculty of Medicine, Charles University Prague

---

Original research

Abstract

Purpose

Investigate whether ^{123}I-ioflupane SPECT (DaT SPECT) has the potential as a marker of basal ganglia damage in acute methanol poisoning.

Methods

Prospective, single-centre, cohort study of patients with confirmed methanol poisoning was conducted. DaT SPECT was performed twice with semi-quantification using DaTQUANT^{TM} and MRI-based volumetry was calculated. Specific binding ratios (SBR) of striatum, caudate nucleus, and putamen were correlated with laboratory parameters of outcome, volumetric data, and retinal nerve fibres layer (RNFL) thickness measurements.

Results

Forty-two patients (mean age 46.3±4.2 y; 8 females), including 15 with putamen lesions (Group I) and 27 patients with intact putamen (Group II), underwent DaT SPECT. Volumetry was calculated in 35 of the patients assessed. SBR values for the left putamen correlated with putamen volume (r=0.665; p<0.001). Decreased bilateral SBR values were determined for the striatum and the putamen, but not for the nucleus caudate, in Group I (p<0.05). A strong correlation was observed between the SBR of the posterior putamen and arterial blood pH (r=0.574; p<0.001) and other toxicological parameters of severity of poisoning/outcome including serum lactate, glucose, and creatinine concentrations (p<0.05). The SBR of the posterior putamen positively correlated with the global RNFL thickness (p<0.05). ROC analysis demonstrated a significant discriminatory ability of SBR of the posterior putamen with AUC=0.753 (95%CI 0.604−0.902; p=0.007). The multivariate regression model demonstrated that arterial blood pH, age, and gender were the most significant factors associated with SBR of the posterior putamen.

Conclusion

DaT SPECT demonstrates significant potential for the diagnosis of methanol-induced basal ganglia damage.

Introduction

Worldwide, methanol is one of the top-five most extensively used chemicals in industry, agriculture, and by consumers as a solvent, antifreeze, cleaning agent, fuel, constituent of windshield washer and brake fluids, and in the production of other chemicals and mixtures [1−3]. Cases of accidental or occupational poisoning with methanol-containing products are reported frequently [4−7]. In 2018, the American Association of Poison Control Centres' National Poison Data System reported 2,192 cases of acute exposure to methanol, including 1,356 that involved exposure to windshield washing solutions, 655 that involved exposure to toxic alcohols containing methanol, 157 cases in which methanol exposure

occurred through use of automotive products, and 24 cases in which individuals were exposed to methanol in cleaning agents [8]. Mass and cluster outbreaks of methanol poisoning as a result of adulterated alcohol consumption have occurred throughout the world in the 21st century, including European countries as Norway, Estonia, Finland, Poland, Italy, and the Czech Republic [9–11].

The high degree of lethality and high rate of long-term health sequelae in survivors exceeding 40% make the treatment of methanol intoxication a challenge for health care providers globally [12–14]. Bilateral necrosis of the basal ganglia, mostly the putamen, with or without haemorrhage, and haemorrhagic lesions in subcortical white matter are typical computed tomography (CT) and magnetic resonance imaging (MRI) findings observed in survivors [15, 16]. Other rare MR findings include necrotic lesions within the globus pallidus, nucleus caudate, thalamus, cerebellum, brainstem, pons and cerebral cortex, and optic nerve atrophy [17–20]. Methanol-induced basal ganglia lesions are associated with secondary parkinsonism, which is characterised by rigidity, dystonia, bradykinesia, mild tremor, masked face, lethargy, and cognitive deficits [21–26]. Other neurological sequelae that result from severe methanol intoxication include transverse myelitis, motor neuron disorder resembling amyotrophic lateral sclerosis, visual anosognosia, and pseudobulbar palsy [27–29]. Chronic retinal neurodegeneration with progressive loss of visual functions is observed in up to 24% of methanol-poisoning survivors [30]. Long-term central nervous system (CNS) and visual sequelae of methanol poisoning are associated with significantly decreased quality of life [31].

MRI-volumetric analysis of the brain has increasingly been used to quantitatively assess changes in different brain structures. Patients with MRI signs of methanol-induced brain damage possess significantly decreased basal ganglia volumes, and the most significant changes occur in the putamen [32]. Basal ganglia neurons and their axons are susceptible to damage induced by hypoxia and oxidative stress [33, 34]. Damaged brain tissue undergoes oedema of affected areas, and later, necrosis, glial scar and postmalatic pseudocyst formation result in decreased brain volume in affected regions [35]. The putamen receives extensive dopaminergic projections from the substantia nigra pars compacta [36]. Altered putaminal volume and shrinkage of the striatum due to decreases in neuronal numbers may affect diverse regions of the brain, since the substantia nigra, thalamus and frontal cortical regions form a topographically organized, cortical-striatal-thalamic-cortical loop [37].

Dopamine transporter (DaT) is a protein that is expressed in the membrane of dopaminergic cells. It facilitates the re-uptake of dopamine into presynaptic terminals. Modern imaging techniques applying ^{123}I-N-v-fluoropropyl-2b-carbomethoxy 3b-(4-iodophenyl)nortropane ([^{123}I]FP-CIT, or ^{123}I-ioflupane) for labelling DaT provide a useful tool for evaluating dopaminergic terminal function by single photon emission computed tomography (DaT SPECT), an established method that has widely been applied in both clinical practice and research [38]. Dopamine transporter imaging is key for diagnosing idiopathic parkinsonism (e.g., Parkinson's disease, multisystem atrophy, progressive supranuclear palsy, Lewy body dementia) to distinguish between the occurrence of nigrostriatal degeneration and the preservation of dopaminergic function in clinically uncertain cases of suspected parkinsonian syndrome.

Striatal DaT binding may contribute to axonal dysfunction or DaT expression in the nigrostriatal pathway in patients acutely exposed to methanol. However, no systematic studies have investigated striatal dopaminergic system integrity via functional imaging in survivors of acute methanol poisoning, and only episodic case reports have been published [39, 40]. Therefore, it remains unclear whether putaminal necrosis in methanol-poisoned patients decreases striatal DaT binding as a result of axonal denervation. The association between volumes of interest (VOI) measurements determined via MRI and specific binding ratios (SBR) determined via 123I-ioflupane on DaT SPECT is unclear. Furthermore, researchers have not identified whether quantitative indices of DaT SPECT are associated with poisoning severity, which is determined using acute toxicological laboratory parameters (e.g. base deficit, serum methanol, formate, lactate, glucose, and creatinine concentrations), prognostic factors (e.g. arterial blood pH, serum ethanol concentration, poisoning severity score, PSS), and hospital treatment modalities [30, 41, 42]. To answer these questions, the relationship between ^{123}I-ioflupane for the striatum, putamen, nucleus caudate SBRs and MRI-based volumes of these brain structures was investigated. The association between DaT SPECT values and the severity of acute methanol poisoning and clinically applied prognostic factors of long-term outcomes was explored.

Materials And Methods

Study design and setting

We carried out a prospective, longitudinal, single-centre, observational cohort study of patients with confirmed acute methanol poisoning that were treated in hospitals during a mass methanol poisoning outbreak that occurred in the Czech Republic from September to December of 2012 [11]. The Institutional Ethics Committee approved the prospective study and written informed consent was obtained from all patients prior to study enrolment. Clinical and laboratory tests indicating acute exposure were collected using standardised data collection protocols. Information regarding treatment modalities used and outcomes was collected from discharge reports. Patients who survived methanol poisoning and were discharged from the hospital were examined 3–8 months and then 2, 4 and 6 years after discharge using the same clinical examination and equipment, hardware and image acquisition, reconstruction, and analysis protocol.

Selection of participants and treatment methods

The national monitoring and reporting system of all cases of acute methanol poisoning was established during the methanol poisoning outbreak. All hospitalised patients with analytically confirmed methanol poisoning were eligible for the study. The patients underwent standard neurological examinations and complete ocular examinations while they were hospitalised and also when they were discharged from the hospital. The examination protocol included either a brain CT or MRI. The patients were considered to have CNS sequelae of acute methanol intoxication if MRI or CT brain scans revealed lesions of the basal ganglia.

Treatment was provided according to the European Association of Poisons Centres and Clinical Toxicologists and the American Academy of Clinical Toxicology guidelines for treatment of methanol poisoning [41]. Alcohol dehydrogenase (ADH) blockers, ethanol and fomepizole, were used as antidotes [43]. Other treatment modalities administered included folate substitution, bicarbonate, enhanced elimination methods, intermittent haemodialysis or continuous veno-venous haemodialysis / haemodiafiltration [44].

Brain imaging protocol and clinical follow-up

During the follow-up, all subjects were scanned using 3T imaging (MAGNE-TOM Skyra; Siemens Healthcare, Erlangen, Germany). The MRI protocol included a T1-weighted 3D MPRAGE sequence for brain volumetry, and the following parameters were applied: repetition time (TR) 2,300 ms, echo time (TE) 2.26 ms, inversion time (TI) 732 ms, slice thickness 1.0/0 mm and flip angle (FA) 8°. Further, sequences were used to describe brain pathology via T2WI, 3D FLAIR, SWI and coronal T2WI with fat saturation was used to visualise optic nerves. All MR data were processed using the MorphoBox prototype software. These data allowed researchers to estimate single brain structure volumes in cm^3. The estimation was calculated in five steps: (i) a brain template was created each input MR using nine-parameter affine spatial transformation (three translational and three rotational parameters followed by anisotropic scaling); (ii) the input image was corrected for bias field using an expectation-maximisation algorithm; (iii) a total intracranial volume (TIV) template mask was resampled and applied to the transformation obtained in step i for skull stripping; (iv) a template-free tissue classification algorithm was used on the TIV-restricted image, which produced three tissue posterior probability maps (grey matter, white matter and cerebrospinal fluid); and (v) the tissue probability maps were combined with the masks that were resampled in the first step to produce regional volume estimates [45, 46].

The follow-up clinical examination protocol, aside from brain MRI and DaT SPECT performed on the same day, included the neurological examination of motor and sensory function, reflexes, cerebellar function, cranial nerves function, and Neuroprotection and Natural History in Parkinson's Plus Syndromes scale, an ophthalmological examination, visual evoked potentials, and optical coherence tomography with retinal nerve fibres layer (RNFL) thickness measurement. RNFL thickness was measured by SD-OCT Spectralis Tracking Laser Tomography (Heidelberg Engineering GmbH, Heidelberg, Germany; software version 5.8.3) and was compared to a normative database. The following biochemical tests were performed: serum glucose, glycohaemoglobin, albumin, prealbumin, liver and renal function tests, lipids, thyroid-stimulating hormone (TSH), vitamins B_1 and B_{12}, carbohydrate-deficient transferrin (CDT), and ethyl glucuronide screening in urine.

DaT SPECT

^{123}I-ioflupane (DATSCAN^{TM}, GE Healthcare, B.V Eindhoven, Netherlands) was used for DaT SPECT. Dosage and scanning procedures were in accordance with the manufacturer's recommendations. Images were acquired using a dual-head SPECT scanner, the GE Infinia HawkEye4 (GE Healthcare, Milwaukee, WI,

USA) equipped with a parallel collimator. Imaging was commenced 3 hours after an intravenous bolus injection of standard activity (185 MBq) of the radiopharmaceutical. The SPECT projections were acquired for 40 s per projection in a 360° stepwise rotation of detectors, with a rotation radius of 15 cm. Data was collected in 128 x 128 matrices with a zoom factor of 1.33, rendering a pixel size of 3.32 x 3.32 mm. Image reconstruction was done with OSEM (2 iterations, 10 subsets) and post-filtered with a Butterworth filter (critical frequency 0.6 cm^{-1}, order 10). The triple energy window technique was applied for scatter correction. The total scanning time of the protocol was 45 min. A representative example of DaT SPECT image is shown in Fig. 1.

Commercially available DaTQUANT^{TM} (GE Healthcare, Little Chalfont, UK) software was used for automatic semi-quantitative image analyses. After SPECT reconstruction, transaxial slices were used as software input, which applies an automatic VOI-based semi-quantitative evaluation of the image data and compares it to an in-built set of reference data for statistical analysis. Pre-defined template VOIs were automatically positioned in the striatum, putamen, and caudate regions in each hemisphere, and in the occipital reference region. The program calculated semi-quantitative SBR as the difference between the mean counts in each VOI and the mean counts in the background, divided by the mean counts in the background.

Statistical analysis

For all variables, basic descriptive statistics (mean, CI, SD, skewness and kurtosis) were calculated, and the data were tested for normality using Shapiro-Wilk's test. The Pearson's c^2 test was used to compare the frequencies of categorical demographic and clinical variables between the groups of methanol poisoning survivors with and without MRI signs of necrotic lesions of the putamen. Continuous variables (volumetric data, SBR, and others) were compared using t-test for independent groups. Bivariate associations were assessed using Pearson's correlation coefficient with the two-tailed significance test option. Reliability analysis was conducted using the intraclass correlation coefficient (ICC) to index the reliability of DaT SPECT measurements in the first and the second examination. The ICC between the two examinations was calculated using the two-way random-effects model for absolute agreement between measurements. A multivariate regression model was used to predict the SBR for the striatum, nucleus caudate, putamen, anterior putamen, and posterior putamen posterior based on several predictors including age, gender, chronic alcohol abuse, smoking, and arterial blood pH at admission. Receiver operating curves (ROC) and the area under the curve (AUC) were used to compare discriminatory capacities of the SBR in different VOI for indicating methanol-induced basal ganglia damage. The best cut-off scores within the ROC analysis were identified in terms of sensitivity and specificity. The level of significance was set to α = 0.05. The statistical analyses were performed using Statistical Product and Service Solutions software (IBM SPSS Statistics for Windows, Version 25.0).

Results

Patient characteristics

Of 108 patients hospitalized with acute methanol poisoning, 84 survived. These survivors were asked whether they would be willing to participate in a study that involved a long-term assessment of the effects of methanol poisoning. Of the 54 patients who agreed, in 42 patients (8 females), brain MRI was performed four times during a six-year period and DaT SPECT was performed twice (four and six years after discharge). The patients had not previously been diagnosed with neurological, neurodegenerative, neurovascular, or psychiatric disorders other than chronic alcohol abuse. In 15/42 patients (36%), brain MRI revealed signs of necrotic lesions of the putamen (patients classified as Group I) and in 27 patients, no signs of putaminal damage were detected (classified as Group II). Focal necrotic lesions in the globus pallidus were found in 6 patients (14%), three of them were members of Group I. Of the 42 patients that had undergone DaT SPECT and MRI of the brain, MRI-volumetry was measured in 35 patients (8 females, p = 0.682), 13 patients with necrotic lesions of the putamen and 22 without signs of putaminal damage (p = 0.897). In seven patients, volumetric measurements were technically unfeasible due to the low quality of primary imaging data.

Demographic, clinical, and MRI-volumetric characteristics of patients on their dates of admission and follow-up laboratory data are summarised in Table 1. The two groups did not differ with respect to age, gender, proportion of chronic alcohol abusers or proportion of smokers when admitted to the hospital with acute methanol poisoning. The patients with MRI-detected necrotic lesions of the putamen tended to be more severely poisoned and have lower arterial blood pH and bicarbonate concentrations. They also tended to have increased base deficit, anion gap, and serum lactate levels, which are characteristics of metabolic acidosis. All patients admitted in a coma belonged to Group I and 80% of the patients with PSS 3 poisoning (severe poisoning) were the group (p < 0.001). No difference in treatment modalities (administration of ethanol versus fomepizole for ADH blocking, folate substitution) and in the follow-up laboratory parameters was observed between the two groups. Patients in Group I had lower left putamen, nucleus caudate, and globus pallidus volumes than those of Group II, but did not display different right VOI, which revealed a degree of asymmetry associated with MRI-volumetric findings (Table 1).

Table 1 Basic demographic, clinical, MRI-volumetric characteristics, admission and follow-up laboratory data of the study population

Characteristic	All patients (n = 42)	Group I (n = 15)	Group II (n = 27)	P
Age (years)	46.3±4.2	45.5±6.0	46.7±5.9	0.778
Males, no. (%)	34 (81)	12 (80)	3 (81)	0.912
Chronic alcohol abuse, no. (%)	31 (74)	9 (60)	24 (89)	0.089
Smoking, no. (%)	22 (52)	8 (53)	14 (52)	0.976
Time, hours	32.1±4.7	30.5±8.9	32.9±6.0	0.643
Coma, no. (%)	7 (17)	7 (47)	0	--
CDT, %	3.8±1.4	3.0±2.5	4.2±1.8	0.405
S-MetOH, mg/L	1380.0±440.0	2020.0±990.0	1010.0±390.0	0.065
S-EtOH, mg/L	250.0±150.0	170.0±180.0	300.0±220.0	0.337
Arterial blood pH	7.17±0.07	6.97±0.11	7.29±0.04	**<0.001**
HCO_{3-}, mmol/L	11.4±2.3	6.2±3.1	14.5±2.6	**<0.001**
Base deficit, mmol/L	16.4±3.4	24.5±5.2	11.5±3.3	**<0.001**
Anion gap, mmol/L	27.7±3.1	33.5±6.4	24.6±3.0	**0.006**
S-Formate, mg/L	590.0±150.0	650.0±280.0	550.0±200.0	0.566
S-Creatinine, mcmol/L	93.0±11.0	112.0±24.0	81.9±7.0	**0.024**
S-Glucose, mmol/L	8.1±1.2	10.4±2.9	6.8±0.7	**0.024**
S-Lactate, mmol/L	3.3±1.3	5.5±2.8	1.7±0.3	**0.015**
PSS 1/2/3, no. (%)	20/8/14 (48/19/33)	2/1/12 (13/7/80)	18/7/2 (67/26/7)	**<0.001**
Antidote (ethanol/fomepizol), no. (%)	30/12 (71/29)	8/7 (53/47)	24/5 (89/11)	0.073
Folate substitution, no. (%)	32 (76)	12 (80)	20 (74)	0.638
GlycHb (%)	34.9±1.9	33.3±2.5	35.8±2.7	0.183
Vitamin B_{12} (mcmol/L)	424.0±75.0	520.0±190.0	371.0±57.0	0.133
Vitamin B_1 (mcmol/L)	57.1±3.6	60.5±7.4	55.3±4.1	0.180
TSH (IU/L)	2.5±0.3	2.6±0.4	2.5±0.4	0.683
Volume of putamen right, cm^3	6.01±0.31	5.68±0.63	6.21±0.35	0.107
Volume of putamen left, cm^3	6.34±0.45	5.58±0.96	6.78±0.39	**0.027**
Volume of nucleus caudate right, cm^3	4.53±0.24	4.41±0.44	4.61±0.30	0.421
Volume of nucleus caudate left, cm^3	4.19±0.21	3.92±0.22	4.35±0.30	**0.022**
Volume of globus pallidus right, cm^3	1.83±0.10	1.80±0.18	1.84±0.12	0.678
Volume of globus pallidus left, cm^3	1.79±0.11	1.66±0.14	1.86±0.15	**0.049**

Notes: Group I – patients with MRI signs of necrotic lesions of the putamen; Group II – patients without MRI signs of necrotic lesions of the putamen; Age – age at admission to the hospital; Coma – admitted in coma to the hospital; Time – time span between methanol exposure and hospital admission; CDT – carbohydrate deficient transferrin; S-MetOH – serum methanol concentration at admission; S-EtOH – serum ethanol concentration at admission; HCO_{3-} - bicarbonate concentration at admission; S-Formate – serum formic acid concentration at admission; PSS -Poisoning severity score; GlycHb – serum glycated haemoglobin; TSH – thyroid-stimulating hormone. MR-volumetry data are presented for 35 patients from the study population. The level of significance is p < 0.05 (bold numbers).

Correlation between mean specific binding ratios on DaT SPECT, clinical and laboratory parameters of poisoning severity and outcomes

There was no difference observed between the two groups with regard to the relative variation of background signals, ruling out significant differences in image quality. An assessment of reproducibility between the first and the second examination revealed strong agreement (intraclass correlation coefficients for the SBR for all VOI ranged from 0.853 to 0.933, all $p < 0.001$). Therefore, mean quantitative indices as the averages of the first and the second measurements were further applied. DaT SPECT results produced significantly lower mean SBR for the whole striatum and for the bilateral putamen, but not for the nucleus caudate, in the patients with necrotic lesions of the putamen detected on brain MRI (Table 2). The greatest difference in the SBR was observed for the bilateral posterior putamen. Certain asymmetry in the SBR for the right and left hemispheres was observed, with lower indices determined for the left putamen, but the difference was not significant ($p > 0.05$).

Table 2 Specific binding ratios (SBR) for the striatum, putamen, and nucleus caudate in survivors of acute methanol poisoning (means with SD)

Variables	All patients (n = 42)	Group I (n = 15)	Group II (n = 27)	P
SBR of the striatum				
Striatum dexter	2.13±0.13	1.96±0.22	2.23±0.15	**0.042**
Striatum sinister	2.12±0.14	1.90±0.29	2.25±0.15	**0.022**
SBR of the putamen				
Putamen dexter	2.00±0.13	1.77±0.22	2.13±0.15	**0.007**
Putamen sinister	1.97±0.15	1.70±0.30	2.12±0.15	**0.017**
SBR of the nucleus caudate				
Nucleus caudate dexter, mean	2.44±0.14	2.40±0.25	2.46±0.18	0.702
Nucleus caudate sinister, mean	2.42±0.15	2.30±0.31	2.49±0.17	0.241
SBR of the putamen anterior				
Putamen anterior dexter, mean	2.15±0.13	1.95±0.24	2.26±0.16	**0.026**
Putamen anterior sinister, mean	2.11±0.14	1.89±0.30	2.23±0.15	**0.023**
SBR of the putamen posterior				
Putamen posterior dexter, mean	1.68±0.13	1.38±0.21	1.85±0.14	**<0.001**
Putamen posterior sinister, mean	1.70±0.16	1.34±0.30	1.90±0.16	**<0.001**

Notes: Group I – patients with MRI signs of necrotic lesions of the putamen; Group II – patients without MRI signs of necrotic lesions of the putamen. The level of significance is $p < 0.05$ (bold numbers).

The SBR for the left putamen was strongly positively correlated with its volume (Fig. 2). Correlations between SBR and the volume of the right putamen were significant only for the posterior putamen ($r = 0.386$, $p = 0.022$). In contrast, the volume of the nucleus caudate was not correlated with its SBR, and the SBR for the striatum and the putamen ($p > 0.05$). Finally, the volume of left, but not right, globus pallidus

positively correlated with the SBR for the whole putamen (r = 0.344, p = 0.043), and for the posterior putamen (r = 0.378, p = 0.025). No correlation was found between the SBR for the whole striatum and the volume of nucleus caudate or globus pallidus (p > 0.05).

The SBR for the striatum, putamen and nucleus caudate in both hemispheres did not correlate with age, gender, and duration between methanol exposure and hospital admission (p > 0.05). There was a significant positive correlation between chronic alcohol abuse and the SBR for the right, but not left, posterior putamen (r = 0.327, p = 0.037; r = 0.286, p = 0.070, respectively). Smokers had higher mean SBR for the whole striatum (r = 0.319, p = 0.042; r = 0.325, p = 0.038 for the right and the left hemispheres, respectively) and for the nucleus caudate (r = 0.327, p = 0.037; r = 0.348, p = 0.026 for the right and the left hemispheres, respectively) than non-smokers. However, SBR for the putamen did not differ significantly between smokers and non-smokers (p > 0.05).

Strong positive correlation was present between arterial blood pH at admission as the main prognostic parameter of poisoning outcome and the SBR for the putamen (r = 0.396, p = 0.012; r = 0.455, p = 0.004 for the right and the left putamen, respectively). The strongest correlation was observed between arterial blood pH and the SBR for posterior putamen posterior bilaterally (Fig. 3). Serum lactate concentration at admission as an indicator of the severity of metabolic acidosis, strongly negatively correlated with the SBR of the putamen bilaterally (r = -0.474, p = 0.006; r = -0.435, p = 0.013 for the right and the left putamen, respectively). These data also showed the strongest correlation for the posterior putamen (r = -0.596, p < 0.001; r = -0.533, p = 0.002, for the right and the left posterior putamen, respectively).

The SBR for the bilateral posterior putamen was negatively associated with acute stress glycaemia (r = -0.504, p = 0.001; r = -0.468, p = 0.002 for right and left posterior putamen, respectively) and with serum creatinine concentration, which is an indicator of acute kidney damage in severely poisoned patients (r = -0.353, p = 0.025; r = -0.350, p = 0.027 for right and left posterior putamen, respectively). Both laboratory parameters reflected poor outcomes of acute methanol poisoning. No correlations between SBR and serum methanol, ethanol, or formic acid concentrations were identified (p > 0.05). Further, no associations were present between the type of antidote administered at the hospital (ethanol or fomepizole), folate substitution, and the SBR for all VOI assessed in our study (p > 0.05).

Follow-up laboratory parameters demonstrated no correlations between glycated haemoglobin, TSH, vitamin B_{12} concentrations, and the SBR for all VOI assessed. However, despite the lack of significant differences between serum vitamin B_1 concentrations of the two groups, they were negatively correlated with the SBR for the putamen (r = -0.314, p = 0.043; r = -0.382, p = 0.013, for right and left putamen, respectively), with the strongest correlation for the SBR of the left putamen posterior (r = -0.421, p = 0.005).

The SBR for the bilateral posterior putamen positively correlated with global and nasal RNFL of the left eyes (for global RNFL: r = 0.358, p = 0.027, and r = 0.376, p = 0.020; for nasal RNFL: r = 0.362, p = 0.025,

and r = 0.382, p = 0.018 for right and left putamen, respectively). However, correlations between SBR and RNFL values of the right eyes were not significant.

Specific binding ratio as the marker of putaminal damage in acute methanol poisoning

ROC and the AUC were used to assess the SBR as an indicator of putaminal damage in survivors of methanol poisoning. ROC analysis of the SBR for the posterior putamen and whole putamen (average of right and left sides) demonstrated a significant AUC of 0.753 (95% CI: 0.604−0.902; p = 0.007) and of 0.746 (95% CI: 0.595−0.897; p = 0.009), respectively (Fig. 4). These data indicated that the SBR for the putamen and specifically for the posterior putamen is potentially a good marker of methanol-induced basal ganglia damage. ROC analyses demonstrated that the AUC for the SBR for the anterior putamen and whole striatum were 0.709 (95% CI: 0.549−0.868; p = 0.027) and 0.702 (95% CI: 0.542−0.863; p = 0.031), respectively. In contrast, the AUC for the SBR of the nucleus caudate was not significant (AUC = 0.563; 95% CI: 0.376−0.750; p = 0.503).

A multivariate regression model demonstrated that arterial blood pH, age at admission to the hospital, and gender were significant association factors for the SBR for the bilateral posterior putamen in survivors of acute methanol poisoning (Table 3). The association of smoking with SBR demonstrated borderline significance for the right, but not left, posterior putamen. The same model was relevant for the whole putamen, but the degree to which arterial blood pH and the age associated with SBR decreased since values of the SBR for the anterior putamen associated to a lesser degree than those for the posterior putamen to laboratory parameters of the severity of methanol poisoning.

Table 3 Summary of association factors for the SBR for the putamen posterior, putamen anterior, and the whole putamen in survivors of acute methanol poisoning

Variable	B	Standard error	Beta	t	Significance	95% CI Lower Bound	Upper Bound
Putamen posterior dexter							
Constant	-5.65	1.99		-2.84	0.008	-9.70	-1.60
Arterial pH	1.04	0.28	0.50	3.64	**0.001**	0.46	1.61
Age	-0.01	0.01	-0.25	-2.06	**0.047**	-0.02	0.00
Gender	0.35	0.14	0.32	2.58	**0.014**	0.07	0.62
Chronic alcohol	0.18	0.14	0.19	1.33	0.193	-0.10	0.47
Smoking	0.22	0.11	0.26	2.10	**0.043**	0.01	0.43
Putamen posterior sinister							
Constant	-8.21	2.35		-3.50	0.001	-12.98	-3.44
Arterial pH	1.42	0.34	0.56	4.23	**0.000**	0.74	2.10
Age	-0.01	0.01	-0.28	-2.42	**0.021**	-0.02	-0.00
Gender	0.49	0.16	0.37	3.10	**0.004**	0.17	0.82
Chronic alcohol	0.15	0.16	0.12	0.93	0.360	-0.18	0.48
Smoking	0.21	0.12	0.20	1.73	0.094	-0.04	0.46
Putamen anterior dexter							
Constant	-1.44	2.31		-0.62	0.537	-6.13	3.25
Arterial pH	0.49	0.33	0.24	1.49	0.145	-0.18	1.16
Age	-0.01	0.01	-0.20	-1.37	0.180	-0.02	0.00
Gender	0.39	0.16	0.36	2.48	**0.018**	0.07	0.71
Chronic alcohol	0.22	0.16	0.22	1.34	0.189	-0.11	0.54
Smoking	0.28	0.12	0.33	2.31	**0.027**	0.03	0.53
Putamen anterior sinister							
Constant	-2.48	2.41		-1.03	0.311	-7.38	2.42
Arterial pH	0.63	0.34	0.28	1.84	0.074	-0.07	1.33
Age	-0.01	0.01	-0.22	-1.58	0.124	-0.02	0.00
Gender	0.39	0.16	0.33	2.38	**0.023**	0.06	0.72
Chronic alcohol	0.24	0.17	0.23	1.45	0.156	-0.10	0.58
Smoking	0.32	0.13	0.35	2.50	**0.017**	0.06	0.58
Putamen dexter							
Constant	-2.79	2.14		-1.30	0.201	-7.15	1.56
Arterial pH	0.67	0.31	0.33	2.18	**0.036**	0.05	1.29
Age	-0.01	0.01	-0.22	-1.64	0.111	-0.02	0.00
Gender	0.37	0.16	0.36	2.57	**0.015**	0.08	0.67
Chronic alcohol	0.20	0.15	0.21	1.35	0.187	-0.10	0.50
Smoking	0.26	0.11	0.32	2.31	**0.027**	0.03	0.49
Putamen sinister							
Constant	-4.47	2.31		-1.94	0.061	-9.17	0.22
Arterial pH	0.91	0.33	0.40	2.76	**0.009**	0.24	1.58
Age	-0.01	0.01	-0.26	-1.97	0.057	-0.02	0.00
Gender	0.43	0.16	0.36	2.74	**0.010**	0.11	0.75
Chronic alcohol	0.22	0.16	0.20	1.34	0.188	-0.11	0.54
Smoking	0.28	0.12	0.30	2.32	**0.026**	0.04	0.53

Notes: CI – confidence interval; Arterial pH – arterial blood pH at admission to the hospital with acute methanol poisoning; Age – age at admission to the hospital; Chronic alcohol – chronic alcohol abuse. The level of significance is $p < 0.05$ (bold numbers).

Discussion

Our study demonstrated that DaT imaging with 123I-ioflupane SPECT is extremely accurate and is capable of distinguishing between the patients with and without methanol-induced basal ganglia damage. These results revealed that the SBR for the putamen was significantly lower in patients with MRI signs of necrotic putaminal lesions and was correlated with volumetric data. DaT SPECT reflects dopaminergic axonal dysfunction in the striatum, whereas MRI-volumetry directly registers the size of relevant brain structures. The SBR for the putamen as the region of interest showed better classification performance compared to the SBR for the whole striatum. Furthermore, the SBR for the putamen was strongly positively correlated with arterial blood pH at admission to the hospital, acute laboratory parameter reflecting the severity of methanol poisoning and main prognostic indicator of hospital outcome [9, 11, 41, 42]. Of all studied VOI, the SBR for the posterior putamen demonstrated highest sensitivity and specificity for detection of methanol-induced basal ganglia damage. Importantly, DaT expression in the posterior putamen was positively associated with RNFL thickness, which is a basic morphological feature of retinal neurodegeneration after acute methanol poisoning [30].

An association exists between striatal ^{123}I-ioflupane uptake and both the number of dopaminergic neurons in the substantia nigra pars compacta and the functional state of those neuron's axon terminals [47, 48]. Outputs of the substantia nigra pars compacta are directed to the spines of dendrites of GABAergic medium spiny neurons in the striatum. Therefore, DaT SPECT, by evaluating the function of dopaminergic terminal axons, provides indirect information on the numbers of surviving GABAergic neurons in the putamen, especially within its posterior part, the caudal putamen, containing motor circuits where the reductions of dopamine transporters are most severe. Our data are in accordance with results of previous studies that revealed the selective vulnerability of the posterior putamen to hypoxic-ischemic brain injury, which researchers determined to be due to vascular and biochemical factors [49]. Further, we observed certain asymmetry in dopaminergic terminal function decrease with relatively lower indices for the SBR for the left striatum. It is interesting that Parkinsonian disease pathology occurs asymmetrically as well, and clinical motor symptoms manifest unilaterally in the early stages of the disease [50].

Common risk factors of poor prognosis in acute methanol poisoning, such as severity of metabolic acidosis with high anion gap, base deficit, serum lactate, and low arterial blood pH [41, 42], were strongly associated with the SBR for the putamen, especially for the posterior putamen, in our cohort of survivors of poisoning. The SBR for the posterior putamen was strongly correlated not only with severity of acidaemia, but also with stress glycaemia and serum creatinine levels upon admission to the hospital, laboratory markers indicating advanced poisoning with toxic brain damage and acute renal failure. Further, while difference in MRI-based volumes of the right putamen between two groups was under the level of significance, SBR indices clearly demonstrated significant decrease of dopaminergic activity in the right putamen in the patients from Group I. Therefore, DaT SPECT may be comparable to, and in certain situations even more accurate marker than MRI-based volumetry with regard to its capacity to identify patients with toxic lesions of the putamen and quantify the scale of damage. One of the reasons is related to the limitations of MRI-volumetry calculations in the patients with striatum shrinkage, with substantially scarred or deformed basal ganglia as a result of glial reparation processes within necrotic

foci. On the other hand, the spatial resolution of SPECT imaging is typically inferior to that of MRI, and partial volume effects or smoothing may prevent SPECT from detecting small focal lesions in the brain of the patients with mild poisoning [51].

Age dependency has been reported for both males and females for DaT SPECT measurements [52]. In the present study, no correlation of the SBR with age and gender was observed. This lack of association can be explained by the relatively homogenous young age of the study population (IQR 35–58 years), small group size, and the capacity of methanol-induced basal ganglia damage to mask age-related DaT decline. Nevertheless, in the multivariate regression model, both age and gender significantly associated with DaT availability in the putamen. This model demonstrated that arterial blood pH at admission most strongly affected DaT SPECT measurements (Table 3). The toxic effect of formic acid, an inhibitor of mitochondrial respiration, depends on the degree of the metabolic acidosis produced: in a highly acidotic environment, formic acid will be more toxic than in a less acidotic one. The dissociation constant of formic acid (pKa) is 3.8, therefore, a pH-drop by 0.3 would double the undissociated formic acid levels and produce significant increases in toxicity. This occurs because only undissociated formic acid crosses the blood-brain barrier and reaches neurons of the basal ganglia [53].

In the current study, no significant differences were observed in the SBR for the nucleus caudate between the patients with and without MRI-signs of basal ganglia damage. Differences in the SBR for the anterior putamen between two groups were smaller than for the posterior putamen. These data may indicate that the anterior portions of the striatum, which are involved in cognitively demanding tasks that require the generation of novel movement sequences, are less vulnerable to acute methanol toxicity than posterior portions that are involved in simple motor functioning.

Treatment modalities applied during hospitalisation with acute methanol poisoning, administration of fomepizole or ethanol to inhibit ADH, and folate substitution as a co-factor of formic acid oxidation, had no association with DaT availability in the striatum. The effect of chronic alcohol abuse on the SBR was not significant; one of the reasons could be the high proportion (74%) of patients with chronic alcohol abuse in the cohort of survivors of methanol poisoning. No differences were observed in follow-up laboratory parameters (glucose, glycated haemoglobin, TSH, vitamins B_1 and B_{12}, and others) of the two groups, which indicated the absence of further confounders affecting DaT availability in the study cohort. Smoking produced an independent effect on the SBR of the putamen in the multivariate regression model. Smoking most significantly affected the anterior portion of the putamen. It has been previously reported that higher putaminal volume was associated with longer lifetime cigarette use and younger age of smoking initiation [54].

Abnormal thickness of RNFL on optical coherence tomography as a result of the toxic effect of formic acid on retinal ganglion cells, followed by chronic retinal neurodegeneration, has been previously reported in survivors of acute methanol poisoning [30, 55]. DaT SPECT measurements revealed a positive correlation between RNFL thickness and the SBR of the posterior putamen. This finding indicates that OCT with RNFL measurement can be used as a reliable, cheap and simple screening method, indicating

the group of methanol-poisoning survivors with possible basal ganglia damage. In this group, DaT SPECT with ^{123}I-ioflupane can be used for verifying the diagnosis.

The current study has several limitations. First, number of study participants who underwent MRI-volumetry was smaller than the number of patients who underwent DaT SPECT. This may have affected correlations between the SBR and volumetry data. Nevertheless, his is the first study that prospectively assessed a homogenous cohort of survivors of acute methanol poisoning from single clinical setting. The patients of the study were subjected to the same study protocol and equipment for six years, and were recruited after a single, mass methanol poisoning event. Brain MRI was performed on all patients to detect the signs of methanol-induced damage. Secondly, patients with MRI data indicative of necrotic lesions of the putamen tended to be younger than those without signs of putaminal damage, differences were not significant. Third, DaT SPECT was not performed on healthy controls for to ethical reasons. The diagnosis of acute methanol poisoning was confirmed via toxicological laboratory analysis in all patients. A reliable diagnosis of long-term CNS sequelae of acute methanol poisoning requires a relatively long follow-up. The strength of the study consisted in its prospective longitudinal character. MRI of the brain was performed, and patients were examined consecutively four times within a six-year period post-discharge from the hospital. For each patient, DaT SPECT was performed twice in the same medical facility using the same camera, hardware, and acquisition/reconstruction protocol to minimize variability.

Conclusion

DaT SPECT with ^{123}I-ioflupane demonstrates high potential for the assessment of dopaminergic function in the striatum, especially within its posterior region, as a valuable diagnostic tool for evaluating long-term CNS sequelae in survivors of acute methanol poisoning. Importantly, DaT SPECT demonstrated high diagnostic correspondence with MRI-volumetry, and the SBR decrease in the striatum correlated with acute laboratory parameters of poisoning severity and prognostic indicators of hospital outcome, which indicated that DaT SPECT has the potential to more accurately identify patients with basal ganglia damage than brain MRI-volumetry. Therefore, DaT SPECT with ^{123}I-ioflupane is useful for diagnosing long-term CNS sequelae of acute methanol poisoning.

Declarations

Ethical approval and consent to participate

The Ethics Committee of the General University Hospital in Prague approved this prospective study, and written informed consent was obtained from all patients before examinations. The approval No. is 31/15.

Consent for publication

Written informed consent was obtained from all patients before examinations.

Availability of supporting data

All data generated or analysed during this study are included in this published article.

Competing interests

The authors declare that they have no competing interests.

Authors´ contributions

The leading principle investigator contributed to study design and conception, data analysis, and interpretation. All authors were involved in data acquisition, contributed to the literature search and the data analysis. All authors had full access to all of the data in the study and contributed to the writing of the report, reviewed it for intellectual content, and approved the submitted version.

References

1. Blug M, Leker J, Plass L, Gunther A. Methanol generation economics; pp. 603–18. In: Bertau M, Offermanns H, Plass L, Schmidt F, Wernicke HJ (eds.) Methanol: The basic chemical and energy feedstock of the future. Asinger's vision today. Springer, 2014; Berlin, Heidelberg.

2. Kemsley J. Methanol's allure. Chemical & Engineering News 2007;85(49):55–9.

3. Olah GA. Beyond oil and gas: The methanol economy. Angewandte Chemie International Edition 2005;44:2636–39.

4. Choi JH, Lee SK, Gil YE, Ryu J, Jung-Choi K, Kim H, et al. Neurological complications resulting from non-oral occupational methanol poisoning. J Korean Med Sci. 2017;32:371–6.

5. Ryu J, Lim K, Ryu D, Lee HW, Yun JY, Kim SW, et al. Two cases of methyl alcohol intoxication by sub-chronic inhalation and dermal exposure during aluminum CNC cutting in a small-sized subcontracted factory. AOEM 2016;28:65.

6. Soysal D, Yersal Kabayegit O, Yilmaz S, Tatar E, Ozatli T, Yildiz B, et al. Transdermal methanol intoxication: a case report. Acta Anaesthesiol Scand. 2007; 51:779–80.

7. Zhang G, Grews K, Wiseman H, Bates N, Hovda KE, Archer J, et al. Application to include fomepizole on the WHO model list of essential medicines. 2015 (3.8.2015). http://www.who.int/selection_medicines/ committees/expert/19/applications/ Fomepizole_4_2_AC_Ad.pdf.

8. Gummin DD, Mowry JB, Spyker DA, Brooks DE, Beuhler MC, Rivers LJ, et al. 2018 Annual Report of the American Association of Poison Control Centers' National Poison Data System (NPDS): 36th Annual Report. Clin Toxicol. 2019;57(12):1220–413.

9. Hovda KE, Hunderi OH, Tafjord AB, Dunlop O, Rudberg N, Jacobsen D. Methanol outbreak in Norway 2002–2004: epidemiology, clinical features and prognostic signs. J Intern Med. 2005;258(2):181–90.

10. Paasma R, Hovda KE, Tikkerberi A, Jacobsen D. Methanol mass poisoning in Estonia: outbreak in 154 patients. Clin Toxicol. 2007;45(2):152–7.

11. Zakharov S, Pelclova D, Urban P, Navratil T, Diblik P, Kuthan P, et al. Czech mass methanol outbreak 2012: epidemiology, challenges and clinical features. Clin Toxicol. 2014;52(10):1013–24.

12. Blanco M, Casado R, Vázquez F, Pumar JM. CT and MR imaging findings in methanol intoxication. Am J Neuroradiol. 2006;27(2):452–4.

13. Vaneckova M, Zakharov S, Klempir J, Ruzicka E, Bezdicek O, Brozova H, et al. Imaging findings after methanol intoxication (cohort of 46 patients). Neuro Endocrinol Letters 2015;36:737–44.

14. Zakharov S, Kotikova K, Vaneckova M, Seidl Z, Nurieva O, Navratil T, et al. Acute methanol poisoning: Prevalence and predisposing factors of haemorrhagic and non-haemorrhagic brain lesions. Basic Clin Pharmacol Toxicol. 2016;119(2):228–38.

15. Anderson CA, Rubinstein D, Filley CM, Stears JC. MR enhancing brain lesions in methanol intoxication. J Comput Assist Tomogr. 1997;21(5):834–6.

16. Kuteifan K, Oesterlé H, Tajahmady T, Gutbub AM, Laplatte G. Necrosis and haemorrhage of the putamen in methanol poisoning shown on MRI. Neuroradiology. 1998;40(3):158–60.

17. Chen JC, Schneiderman JF, Wortzman G. Methanol poisoning: bilateral putaminal and cerebellar cortical lesions on CT and MR. J Comput Assist Tomogr. 1991;15(3):522–4.

18. Halavaara J, Valanne L, Setala K. Neuroimaging supports the clinical diagnosis of metanol poisoning. Neuroradiology 2002;44(11):924–8.

19. Sefidbakht S, Rasekhi AR, Kamali K, Borhani Haghighi A, Salooti A, Meshksar A, et al. Methanol poisoning: acute MR and CT findings in nine patients. Neuroradiology 2007;49(5):427–35.

20. Vaneckova M, Zakharov S, Klempir J, Ruzicka E, Bezdicek O, Liskova I, et al. Methanol intoxication on magnetic resonance imaging. Cesk Slov Neurol N. 2014;77/110(2):235–9.

21. Anderson TJ, Shuaib A, Becker WJ. Neurologic sequelae of methanol poisoning. Can Med Assoc J. 1987;136(11):1177–9.

22. Bezdicek O, Michalec J, Vaneckova M, Klempir J, Liskova I, Seidl Z, et al. Cognitive sequelae of methanol poisoning involve executive dysfunction and memory impairment in cross-sectional and long-term perspective. Alcohol 2017;59:27–35.

23. Galvez-Ruiz A, Elkhamary SM, Asghar N, Bosley TM. Visual and neurologic sequelae of methanol poisoning in Saudi Arabia. Saudi Med J. 2015;36(5):568–74.

24. LeWitt PA, Martin SD. Dystonia and hypokinesis with putaminal necrosis after methanol intoxication. Clin Neuropharmacol. 1988;11(2):161–7.

25. Oliveras Ley C, Gali G. Parkinsonian syndrome after methanol intoxication. Eur Neurol. 1983;22(6):405–9.

26. Reddy NJ, Sudini M, Lewis LD. Delayed neurological sequelae from ethylene glycol, diethylene glycol and methanol poisonings. Clin Toxicol. 2010;48(10):967–73.

27. Chiò A, Herrero Hernandez E, Mora G, Valentini C, Discalzi G, Pira E. Motor neuron disease and optic neuropathy after acute exposure to a methanol-containing solvent mixture. Amyotroph Lateral Scler Other Motor Neuron Disord. 2004;5(3):188–91.

28. McLean DR, Jacobs H, Mielke BW. Methanol poisoning: a clinical and pathological study. Ann Neurol. 1997;8(2):161–7.

29. Santos-Garcia D, Lopez-Dequidt IA, Exposito-Ruiz I, Fraga-Bau A, de la Fuente-Fernandez R. [Anton's syndrome due to occipital necrosis after methanol poisoning]. Rev Neurol. 2015;60(2):90 [Article in Spanish].

30. Nurieva O, Diblik P, Kuthan P, Sklenka P, Meliska M, Bydzovsky J, et al. Progressive chronic retinal axonal loss following acute methanol-induced optic neuropathy: four-year prospective cohort study. Am J Ophth. 2018;191:100–15.

31. Rulisek J, Waldauf P, Belohlavek J, Balik M, Kotikova K, Hlusicka J, et al. Health-related quality of life determinants in survivors of a mass methanol poisoning outbreak: six-year prospective cohort study. Clin Toxicol. 2020;8:1-11. doi: 10.1080/15563650.2019.1702994.

32. Hlusicka J, Mana J, Vaneckova M, Kotikova K, Diblik P, Urban P, et al. MRI-based brain volumetry as a biomarker of outcomes in acute methanol poisoning. NeuroToxicology 2020 (submitted).

33. Blanco M, Casado R, Vazquez F, Pumar JM. CT and MR imaging findings in methanol intoxication. Am J Neuroradiology 2006;27(2):452–4.

34. Zakharov S, Kotikova K, Nurieva O, Hlusicka J, Kacer P, Urban P, et al. Leukotriene-mediated neuroinflammation, toxic brain damage, and neurodegeneration in acute methanol poisoning. Clin Toxicol. 2017;55(4),249–59.

35. Viola A, Stvrtina S, Bauer V, Zaviacic M. Morphologic and clinical sequelae of focal ischemic lesions. Ceskoslovenska patologie 2000;36(4):140–5.

36. Luo X, Mao Q, Shi J, Wang X, Li CR. Putamen gray matter volumes in neuropsychiatric and neurodegenerative disorders. World J Psychiatry Ment Health Res. 2019;3(1).

37. Haber SN. Corticostriatal circuitry. Dialogues Ckin Neurosci. 2016;18(1):7–21.

38. Darcourt J, Booij J, Tatsch K, Varrone A, Vander Borght T, Kapucu OL, et al. EANM procedure guidelines for brain neurotransmission SPECT using (123)I-labelled dopamine transporter ligands, version 2. Eur J Nucl Med Mol Imaging. 2010 Feb;37(2):443–50.

39. Doe de Maindreville A, Bakchine S, Papathanassiou D, Orquevaux P, Tranchant C, Roze E. Evidence of presynaptic dopaminergic dysfunction in acute methanol intoxication. Rev Neurol (Paris). 2017;173:420–2.

40. Airas L, Paavilainen T, Marttila RJ, Rinne J. Methanol intoxication-induced nigrostriatal dysfunction detected using 6-[18F]fluoro-L-dopa PET. Neurotoxicology. 2008;29:671–4.

41. Barceloux DG, Bond GR, Krenzelok EP, Cooper H, Vale JA. American Academy of Clinical Toxicology practice guidelines on the treatment of methanol poisoning. J Toxicol Clin Toxicol. 2002;40(4):415–46.

42. Paasma R, Hovda KE, Hassanian-Moghaddam H, Brahmi N, Afshari R, Sandvik L, et al. Risk factors related to poor outcome after methanol poisoning and the relation between outcome and antidotes – a multicenter study. Clin Toxicol. 2012;50(9):823–31.

43. Zakharov S, Pelclova D, Navratil T, Belacek J, Komarc M, Eddleston M, et al. Fomepizole versus ethanol in the treatment of acute methanol poisoning: comparison of clinical effectiveness in a mass poisoning outbreak. Clin Toxicol. 2015;53(8):797–806.

44. Zakharov S, Pelclova D, Navratil T, Belacek J, Latta J, Pisar M, et al. Efficiency of acidemia correction on intermittent versus continuous hemodialysis in acute methanol poisoning. Clin Toxicol. 2017;55(2):123–32.

45. Mana J, Vaneckova M, Klempíř J, Lišková I, Brožová H, Poláková K, et al. Methanol poisoning as an acute toxicological basal ganglia lesion model: evidence from brain volumetry and cognition. Alcohol Clin Exp Res. 2019 Jul;43(7):1486–97.

46. Schmitter D, Roche A, Maréchal B, Ribes D, Abdulkadir A, Bach-Cuadra M, et al. An evaluation of volume-based morphometry for prediction of mild cognitive impairment and Alzheimer's disease. NeuroImage: Clinical 2015;7(1):7–17.

47. Colloby SJ, McParland S, O'Brien JT, Attems J. Neuropathological correlates of dopaminergic imaging in Alzheimer's disease and Lewy body dementias. Brain 2012;135:2798–808.

48. Kordower JH, Olanow CW, Dodiya HB, Chu Y, Beach TG, Adler CH, et al. Disease duration and the integrity of the nigrostriatal system in Parkinson's disease. Brain 2013;136:2419–431.

49. Shankaran S, Niimura K, Muzik O, Chugani D, Mantaring J, Kumar P, et al. Selective vulnerability of posterior putamen on positron emission tomography (pet) in perinatal hypoxic-ischemic brain injury. Pediatric Research 1999;45:347.

50. Okuzumi A, Hatano T, Kamagata K, Hori M, Mori A, Oji Y, et al. Neuromelanin or DaT-SPECT: which is the better marker for discriminating advanced Parkinson's disease? Eur J Neurol. 2019;26(11):1408–

16.

51. Jakobson Mo S, Axelsson J, Jonasson L, Larsson A, Ögren MJ, Ögren M, et al. Dopamine transporter imaging with [18F]FE-PE2I PET and [123I]FP-CIT SPECT-a clinical comparison. EJNMMI Res. 2018;8(1):100.

52. Varrone A, Dickson JC, Tossici-Bolt L, Sera T, Asenbaum S, Booij J, et al. European multicentre database of healthy controls for [123I]FP-CIT SPECT (ENC-DAT): age-related effects, gender differences and evaluation of different methods of analysis. Eur J Nucl Med Mol Imaging. 2013;40:213–27.

53. Zakharov S, Kurcova I, Navratil T, Salek T, Pelclova D. Is the measurement of serum formate concentration useful in the diagnostics of acute methanol poisoning? A prospective study of 38 patients. Basic Clin Pharmacol Toxicol. 2015;116(5):445–51.

54. Das D, Cherbuin N, Anstey KJ, Sachdev PS, Easteal S. Lifetime cigarette smoking is associated with striatal volume measures. Addict Biol. 2012;17(4):817–25.

55. Nurieva O, Hubacek JA, Urban P, Hlusicka J, Diblik P, Kuthan P, et al. Clinical and genetic determinants of chronic visual pathway changes after methanol-induced optic neuropathy: four-year follow-up study. Clin Toxicol. 2019;57(6):387–97.
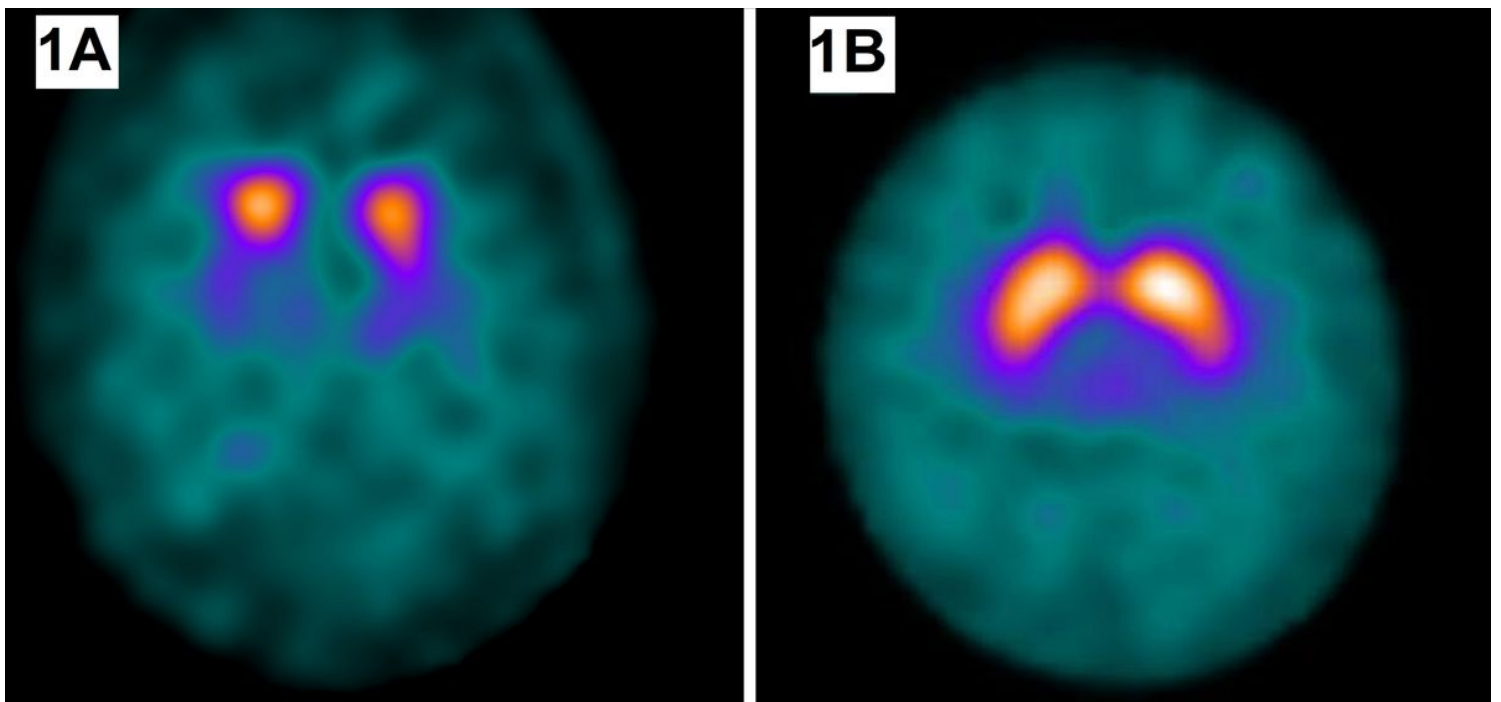
Figures

Figure 1

Example of DaT SPECT image in the patient with severe (a) and minor methanol poisoning (b)
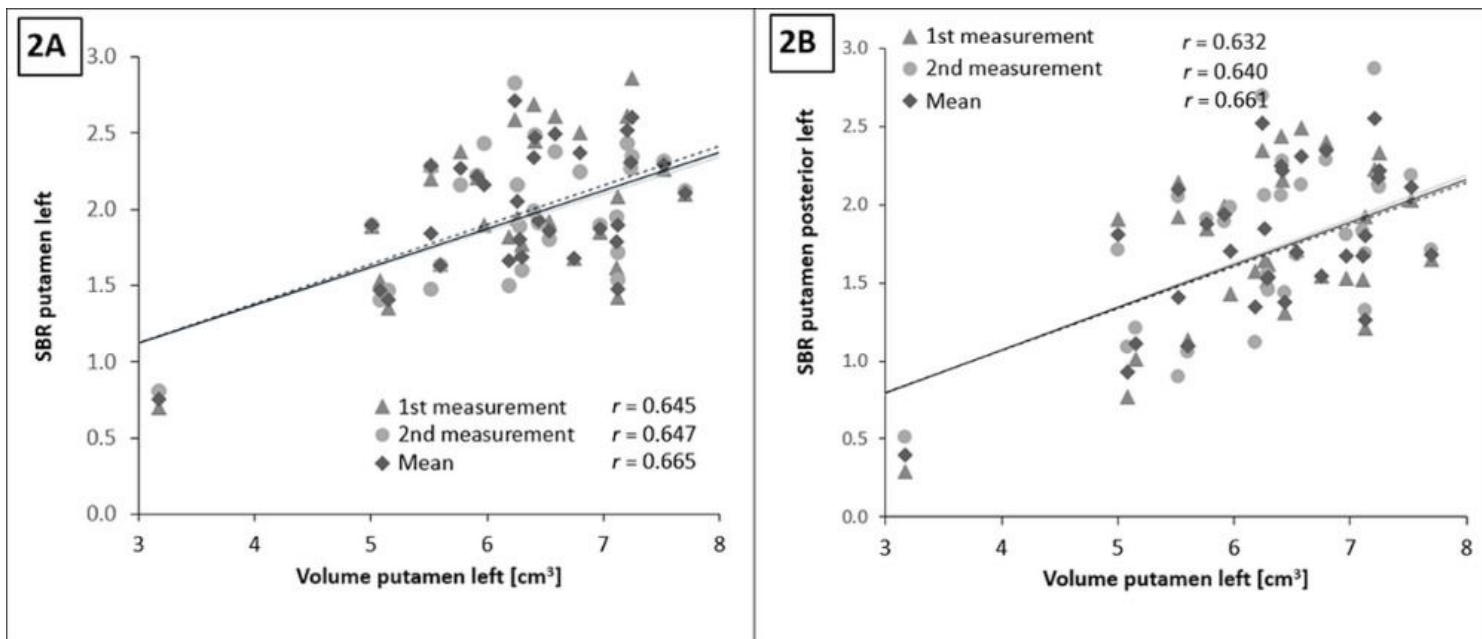
Figure 2

Correlation between SBR on DaT SPECT and volumes of the left putamen (a) and posterior putamen (b)
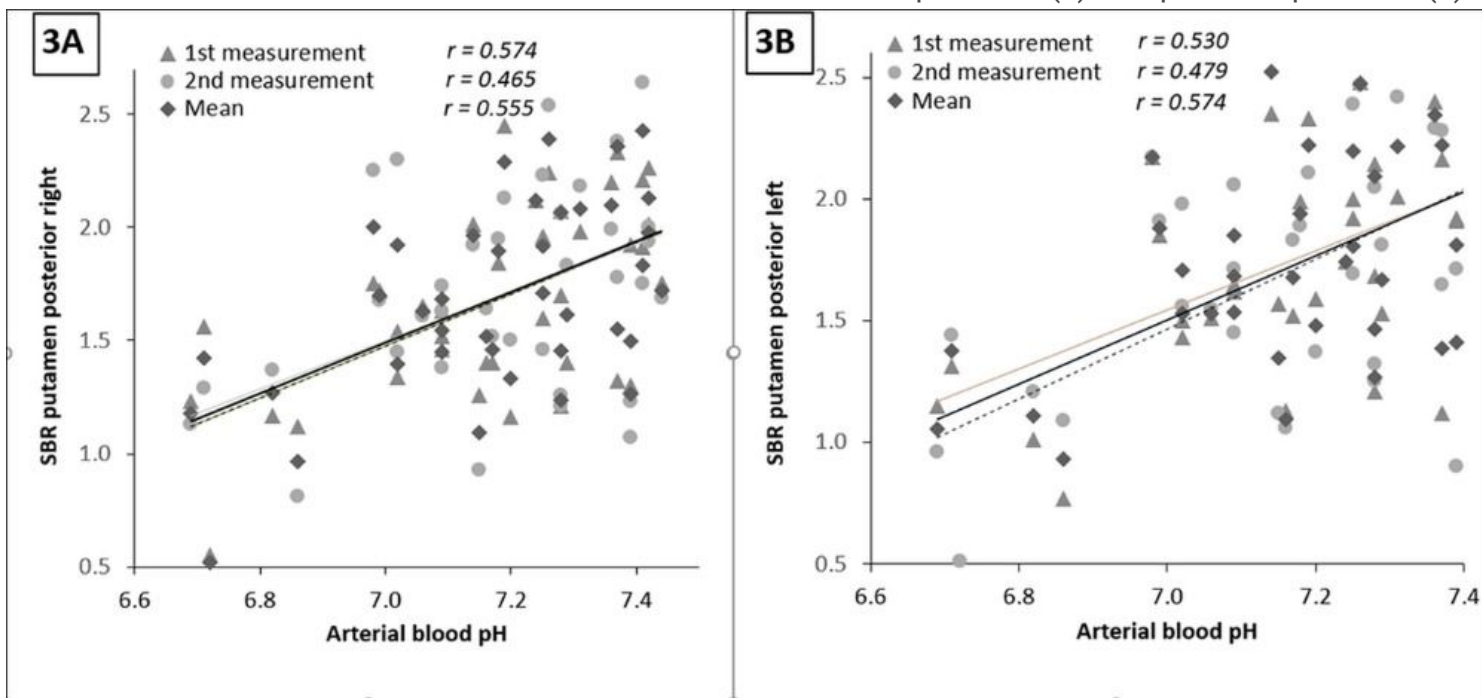

Figure 3

Correlation between arterial blood pH at admission as the main prognostic parameter of poisoning outcome and the SBR for the right (a) and left (b) posterior putamen
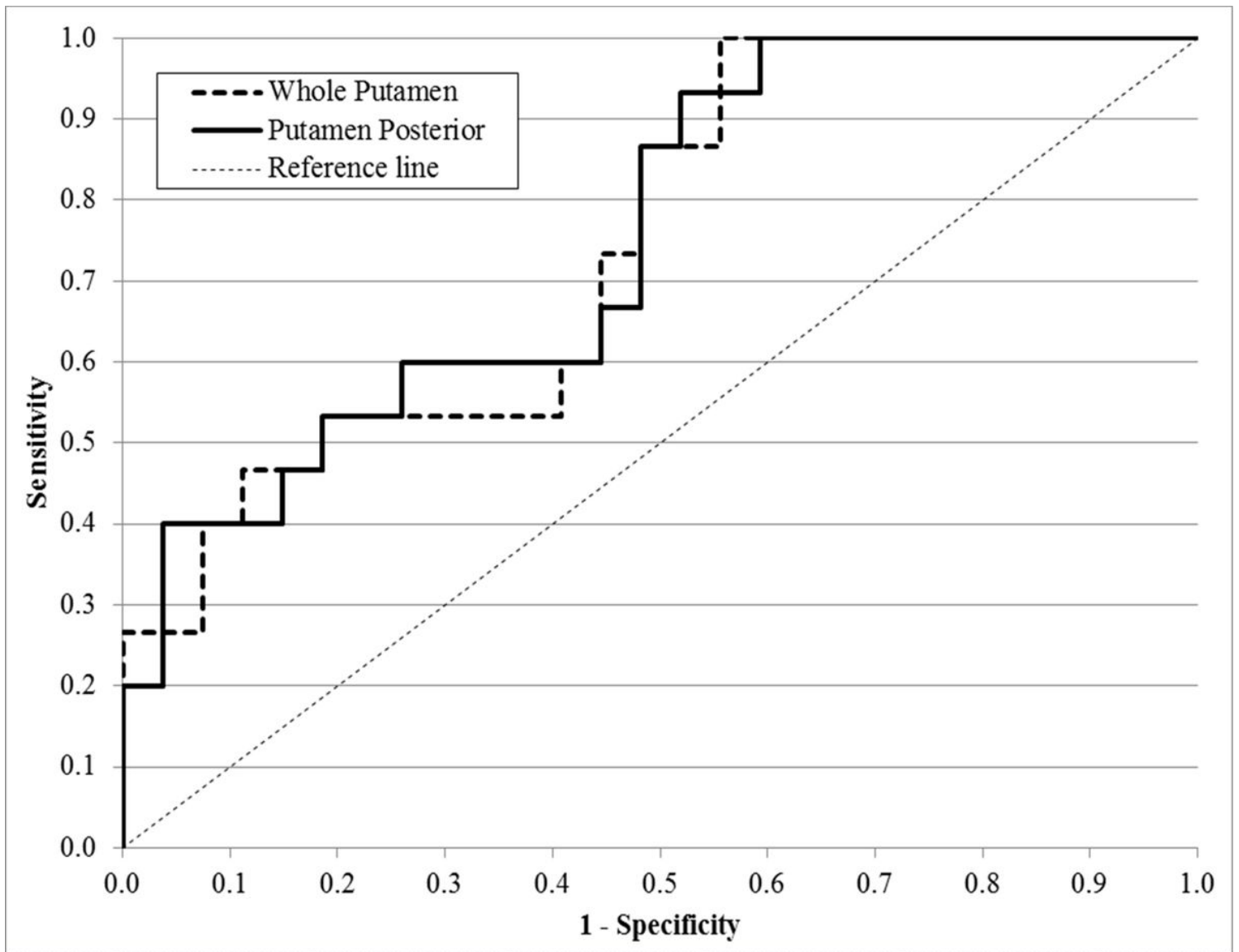
Figure 4

ROC curve analysis of the SBR for the putamen as an indicator of the basal ganglia damage in survivors of methanol poisoning